

## Post earthquake performance monitoring of a typical highway overpass bridge

A. Iranmanesh, A. Bassam and F. Ansari\*

*Department of Civil and Materials Engineering, University of Illinois at Chicago, 2095 Engineering Research Facility, 842 W. Taylor Street (M/C 246), Chicago, Illinois 60607-7023, U.S.A.*

*(Received August 19, 2008, Accepted October 10, 2008)*

**Abstract.** Bridges form crucial links in the transportation network especially in high seismic risk regions. This research aims to provide a quantitative methodology for post-earthquake performance evaluation of the bridges. The experimental portion of the research involved shake table tests of a 4-span bridge which was subjected to progressively increasing amplitudes of seismic motions recorded from the Northridge earthquake. As part of this project, a high resolution long gauge fiber optic displacement sensor was developed for post-seismic evaluation of damage in the columns of the bridge. The nonlinear finite element model was developed using Opensees program to simulate the response of the bridge and the abutments to the seismic loads. The model was modified to predict the bent displacements of the bridge commensurate with the measured bent displacements obtained from experimental analysis results. Following seismic events, the tangential stiffness matrix of the whole structure is reduced due to reduction in structural strength. The nonlinear static push over analysis using current damaged stiffness matrix provides the longitudinal and transverse ultimate capacities of the bridge. Capacity loss in the transverse and longitudinal directions following the seismic events was correlated to the maximum displacements of the deck recorded during the events.

**Keywords:** bridges; columns; nonlinear finite element; damage assessment; earthquakes; fiber optic sensors.

---

### 1. Introduction

Over the past decade, the development and application of performance-based seismic design concepts have gained popularity. Incorporation of performance-based seismic design in modern codes requires establishment of deterministic procedures for assessment of structural damage. Structural performance of a concrete bridge during strong earthquakes is complex and highly nonlinear. Hence a robust computer simulation model with appropriate material properties and robust methodologies plays an important role in reliability of the damage estimations (ATC 2006a, Applied Technology Council 2005b).

In order to properly evaluate the condition of the bridges in the aftermath of earthquakes and to address both safety as well as serviceability concerns, it is essential to develop deterministic methodologies that would go beyond visual inspections (Buckle 1994). These methods will be necessary to assess the severity and level of damage, to establish repair strategies, and to make timely decisions pertaining to the lifelines and traffic patterns (Ansari 2005).

The primary objective of this article is to demonstrate the applicability of Finite Element simulations

---

\*Corresponding Author, E-mail: [fansari@uic.edu](mailto:fansari@uic.edu)

for prediction of damage in a typical concrete bridge. The concrete bridge utilizes degrading nonlinear concrete material model under progressively increasing ground motions. Appropriate material modeling in the computer simulations asks for consideration of continuum damage concepts. In the continuum damage context the elastic, plastic and damaging components are distinguished in the material model (Chaboche 1988). Elemental level damage process decreases the strength and stiffness properties at the materials level, which will eventually manifest itself globally with changes in the structure's stiffness matrix. (Krätzig and Petryna 2005).

A quantifiable criterion that can be used to evaluate a damaged bridge is the probability of its complete collapse in an aftershock (Luco, *et al.* 2004). Computing this collapse probability can be accomplished by obtaining the residual capacity of the damaged bridge to withstand aftershock shaking. The residual capacity can be computed via nonlinear structural analyses utilizing damaged global stiffness matrix of the structure following each event. The residual capacity can be computed by considering the experimental results of the dynamic test to provide a meaningful quantified damage measure.

To accomplish these objectives, a novel fiber optic sensor was developed at the University of Illinois at Chicago (UIC) for monitoring of the severe displacements and crack opening displacements which is normally experienced by the columns during seismic motions. The network of serially multiplexed fiber optic sensors was externally adhered to the sections of the bridge columns with potential for development of plastic hinges. The bridge was tested at the University of Nevada's (UNR) NEES shaking table facility under a NEES grant from the National Science Foundation. This bridge was built by the UNR researchers and UIC's structural health monitoring activities were conducted in parallel with UNR's experiments. Numerical analysis of damage was performed in OpenSees<sup>1</sup> (McKenna and Fenves 2000) and then validated with experimental response.

## 2. Experimental program

The bridge was a quarter scale model of a typical four-span highway bridge and constructed in accordance with the provisions of the National Cooperative Highway Research Program (ATC/MCEER 2001) by the UNR researchers (Nelson, *et al.* 2007). The bridge deck was supported by three piers and two abutments. The piers were each secured on a  $4.3 \times 4.3$  m shaking table. The shaking tables had a force rating of 734 kN; a maximum dynamic displacement range of +300 mm, and a maximum velocity and acceleration ratings of +1270 mm/sec and 1 g at 45.352 tons, respectively.

Bridge dimensions are schematically shown in Fig. 1. The concrete in bridge columns had a compressive strength ( $f'_c$ ) of 48 MPa. The columns were reinforced with sixteen 9.5 mm diameter longitudinal bars with a yield stress,  $f_y$  of 486 MPa, and 4.87 mm diameter spiral reinforcement spaced at 31.75 mm ( $f_y = 424$  MPa).

The length scale of 1/4 relative to the full scale prototype was chosen based on the test set-up capacity. External masses were placed on the bridge deck to mimic scaled axial loads on the columns. Fig. 2 is a photo of the test setup with the bridge on the shaking tables. The experimental program comprised of 13 tests over a period of four days. The experiments involved application of pre-programmed seismic motions to the bridge through the shaking tables. Table 1 provides the peak accelerations and the percent intensity of the Northridge earthquake accelerations used in the experiments (indicated by  $\times$  full scale). The experiments included both single-axes as well as dual-axis

---

<sup>1</sup>Open System for Earthquake Engineering Simulation

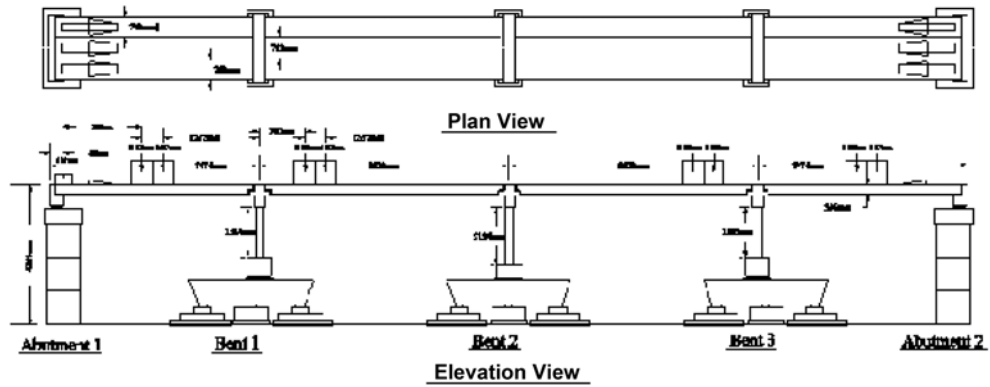


Fig. 1 Bridge dimensions



Fig. 2 Bridge on the shaking tables

Table 1 Bridge input earthquake amplitudes

Event	Test Type	× full scale	PGA (g)	
			Transverse	Longitudinal
1A	W/Restrainer1	0.15	---	0.09
1B	W/Restrainer2	0.15	---	0.09
1C	Longitudinal	0.15	---	0.09
1D	Biaxial	0.15	0.075	0.09
2	Biaxial	0.30	0.15	0.18
3	Biaxial	0.50	0.25	0.3
4A	W/Restrainer1	1.0	---	0.6
4B	W/Restrainer2	1.0	---	0.6
4C	Longitudinal	1.0	---	0.6
4D	Biaxial	1.0	0.5	0.6
5	Biaxial	1.50	0.75	0.9
6	Biaxial	2.0	1	1.2
6R	Biaxial	2.0	1	1.2

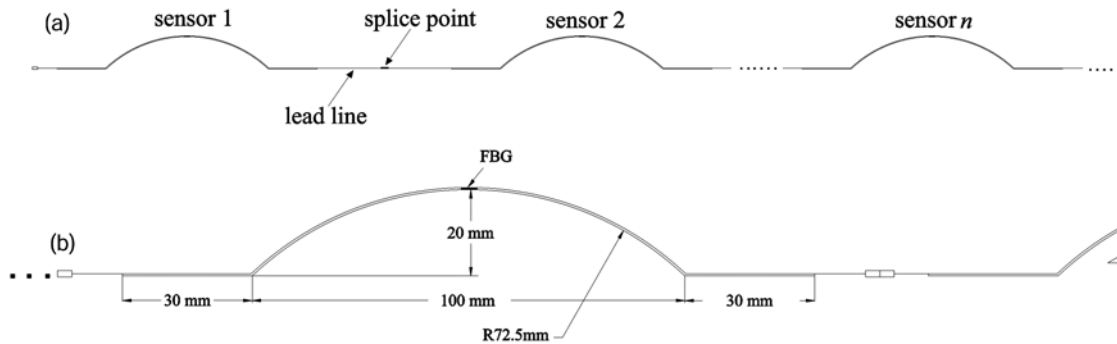


Fig. 3 Fiber optic sensors, (a) Schematics of the serially multiplexed sensors, (b) Sensor dimensions

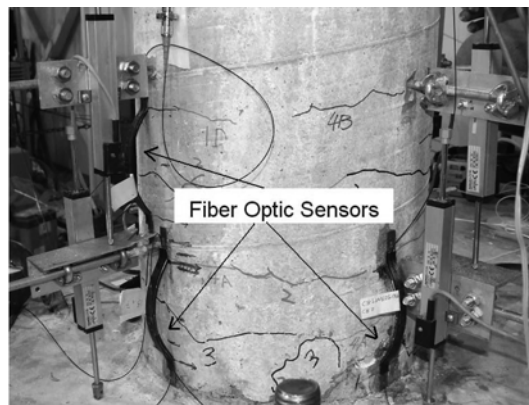


Fig. 4 Fiber optic displacement sensors for monitoring the column curvatures

seismic motions along the longitudinal and transverse directions of the bridge. The time scale of these motions was modified by a factor of 2 to account for the scaling of the bridge prototype.

### 2.1. Sensors and instrumentation

Monitoring of the column curvatures was achieved by instrumenting two bridge bents with surface adhered fiber optic Bragg grating sensors (FBG). The strain transduction mechanism in FBG sensors is based on the shift in the central wavelength of the Bragg gratings (Ansari 2007). The sensors measured the column deformations over 100 mm gauge lengths. Fiber optic sensors were chosen over other types of sensors in order to take advantage of their high resolution and signal to noise ratio, as well as immunity to the electrical and magnetic interferences in the laboratory from other devices and systems. Moreover, it was desirable to limit the number of sensor leads from the bridge to a minimum in these experiments and fiber optics provided the capability for serial splicing of several sensors on one lead-line (Fig. 3a). The columns were expected to crack at the plastic hinge zones and for this reason the FBG sensor assembly (package) was designed to withstand the large dynamic deformation reversals, and with capability for measuring large crack opening displacements (i.e. 10 mm). To achieve this, the sensor assembly was packaged with high strength spring with the FBG as the sensing element (Fig. 3b). By using this approach, the dynamic range of the sensor was mechanically increased (0-10 mm). The

sensor sensitivity was obtained as 650 picometer/millimeter, with the operating temperature of -40–80 degrees C. Up to six sensors were serially multiplexed on a lead line.

Fig. 4 shows the sensors on the bridge column. More sensors were used in the transverse direction since more damage was expected to occur in that direction. The longitudinal and transverse displacements were also measured at the top of the column bents by using string displacement transducers. These displacements agree well with the displacements which were acquired indirectly from the fiber optic sensors.

### 3. Finite element modeling

#### 3.1. Geometric model

The bridge model consists of three-dimensional assemblage of nodes and line elements in the OpenSees Finite Element code. Two types of elements were employed in for modeling, namely linear and nonlinear beam-columns as well as zero length elements for connections.

#### 3.2. General assumptions

All the imposed scaling masses were assumed to be lumped on the deck nodes. Basically due to scaling effects, the axial loads in the modeled bridge columns were smaller than the one in the prototype bridge. Scaling masses were placed on top of the deck to provide required axial forces in the columns (Bazant 2005). It is assumed that column bases are rigidly attached to the foundation such that they can be modeled as fixed connections. The second order P-Delta effects are considered in the analysis. Damping is included in the model using mass and stiffness proportional coefficients that are calculated for two percent damping at the first and third modes.

#### 3.3. Material models

The uniaxial material model selected for concrete in this analysis referred to as the Kent-Scott-Park model with degrading linear unloading/reloading stiffness on the basis of the work reported by Karsan and Jirsa (1969). The 28 day compressive strength of the concrete used for construction of the bridge was 5 ksi (34.5 MPa) as reported by Zadeh and Saiidi (2007). The average strains at peak stress and at the ultimate strength of the 28 day concrete were 0.002 and 0.006, respectively. For the confined concrete the material model parameters were calculated based on Mander's model (Mander, *et al.* 1988), with 6.56 ksi (45.2 MPa) peak stress at 0.005 strain and 5.1 ksi (35.1 MPa) stress at the ultimate strain of 0.0169.

The Giuffré-Menegotto-Pinto Model with Isotropic Strain Hardening was selected for cyclic response of steel in the plastic regime. This material model was employed to build a uniaxial steel material behavior with isotropic strain hardening. This model also has the capability for transition from elastic to plastic regimes. The reinforcing steel bars were modeled using a bi-linear curve with an initial slope of 29000 ksi (199810 MPa), yielding stress of 68 ksi (469 MPa), and the hardening slope of 212 ksi (1461 MPa) (Mazzoni, *et al.* 2005). The tensile and compressive behaviors of these bars were considered symmetrically the same. Bond-slip behavior in the columns was considered thru a non-linear rotational spring connected to the column ends using the procedure described by Wehbe and Saiidi (2003).

All of the superstructure elements were considered uncracked as per design requirements (ATC/MCEER 2001). Hence, the post-tensioned deck and the T-section beams between the deck panels were modeled with linear elastic elements. The column caps were also modeled using linear elastic elements as they were also assumed not to crack. The linear elastic elements applied for this purpose were considered to have gross section properties using the unconfined concrete properties at the 28-day cylinder strength.

### 3.4. Column elements configurations

All of the columns had circular sections with 12 in (304.8 mm) diameter. They were reinforced longitudinally by 16 number 3 steel bars with 0.5 in (12.7 mm) concrete cover. Force-based fiber-section elements with distributed plasticity referred to as Nonlinear-Beam-Column elements were used to model the bridge columns. Three different fiber-element types representing concrete core, steel reinforcement and concrete cover are used in the column fiber-section. A fiber-section with 8 slices, 7 layers of core, and 2 layers of cover was chosen for the analysis. The integration along the element is based on Gauss-Lobatto quadrature rule, with two integration points at the element ends (Davis and Rabinowitz 1984).

### 3.5. Integration method

Different time-steps starting from 0.001 to 0.0001 were applied to obtain convergence for the various events. The Newmark  $\beta$  method (Newmark 1959) was used for the analysis. The profile solver in the program was based on variable bandwidth elimination algorithm providing an efficient solution for large structures.

### 3.6. Bridge-Abutment interaction model

The bridge decks at the two ends were seated on the L-shaped abutment seats on the upper part of the abutment back walls. There was a 0.5 in gap between the vertical surface of the abutment seat and the bridge deck. To simulate a roller type connection, the bridge decks at both ends were seated on frictionless Teflon sheets mounted on the top of the horizontal surfaces of the abutment seats (Zadeh and Saiidi 2007). The abutment seats were connected to the horizontal actuator at each bridge end. The actuators simulated the interaction of soil and back wall during the earthquake motion. The actuators were programmed to exert reactive forces to the bridge deck when the gap between the deck and the vertical surface of the abutment closed during the cyclic load reversals (Nelson, *et al.* 2007). The gap was modeled by a zero-length element with compression-only gap material properties and initial gap size of 0.5 inch. The recorded abutment displacements time history during the events was applied to one node of the gap element.

### 3.7. Input seismic ground motions

Input ground motions to the bridge pertained to the recorded Northridge earthquake accelerations. The ground motions were applied in a number of successively increasing steps in amplitude. These motions were applied to the bridge bases through 3 shaking tables simultaneously in the longitudinal and horizontal directions. The longitudinal peak acceleration during event 1A was 0.09 g and increased

gradually to 1.6 g ending at event 6R. In a similar manner, transverse peak accelerations varied from 0.075 g in event 1D to 1.33 g successively to event 6R. In order to take into account the accumulation of damage following each event, successive analysis of the bridge from event 1A through 6R included the effects of all previous input motions.

#### 4. Validation of the finite element model

Validation of the finite element simulation was accomplished on the basis of post-seismic analysis of the results from the shake table tests. Typical displacement response of the bents as measured by the wire transducers and the simulated results are compared in Figs. 5 and 6. Results shown in Figs. 5-6 pertain to various events at the earlier as well as later seismic events (events 1D, 4D, and 6R). Similar results were obtained for all other events. For all practical purposes, the simulated results match the actual response rather well.

##### 4.1. Post-event analysis

The residual capacity against collapse of a bridge that has been damaged by the main shock can be coupled with the aftershock motion demands to make an objective decision regarding the probability of collapse during an aftershock (Luco, *et al.* 2004). For this bridge a nonlinear static-pushover approach was employed to compute the ultimate capacity of the bridge following each event. The pushover analysis was performed both for the longitudinal as well as the transverse directions. For both directions the bridge deck was pushed till a certain amount of displacement was reached. According to the experimental results, the lateral reinforcement provisions were adequate to prevent longitudinal bar buckling in the plastic hinge regions until the loading event number 6R. At this point, rebars in the

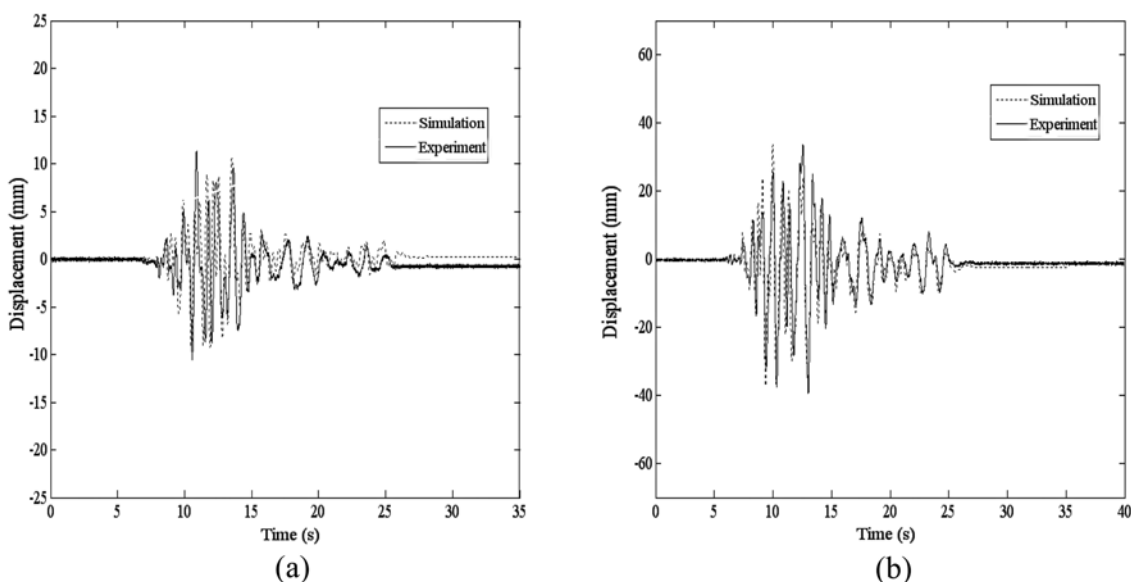


Fig. 5 (a) Comparison of longitudinal displacement from FEM and experiment (event 1D) (b) Comparison of transverse displacement from FEM and experiment (event 4D)

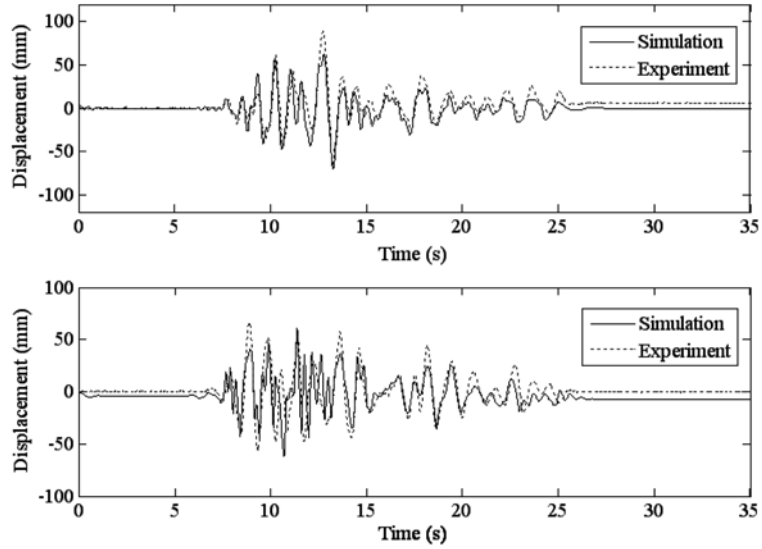


Fig. 6 Comparison of longitudinal and transverse displacement from FEM and experiment in the middle bent (event 6R)

columns of the first bent buckled due to the fracture of lateral reinforcements. Bents 2 and 3 retained lateral load carrying capacity in spite of failure in Bent 1, and provided adequate redundancy to prevent the bridge from collapse. Therefore the ultimate lateral capacity was assumed to occur when the rebars in two bents out of the three reached their rupture strain. Therefore, under these circumstances the bridge becomes unstable and will not be able to sustain resistance against any lateral excitations (Nelson 2007).

The pushover analysis results for the transverse and longitudinal loading directions are shown in Figs. 7 and 8, respectively. These results include all the loading events and therefore, the peaks progressively shift to the right for successive loading events. This is due to the weakening of the bridge following

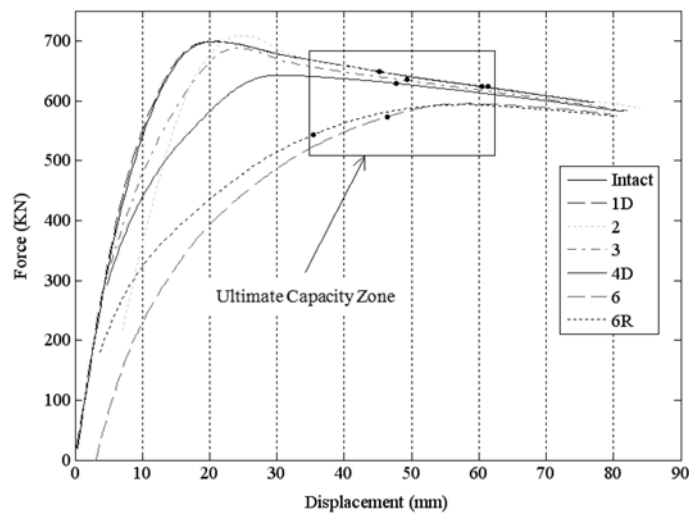


Fig. 7 Pushover curves of the bridge in transverse direction following each event

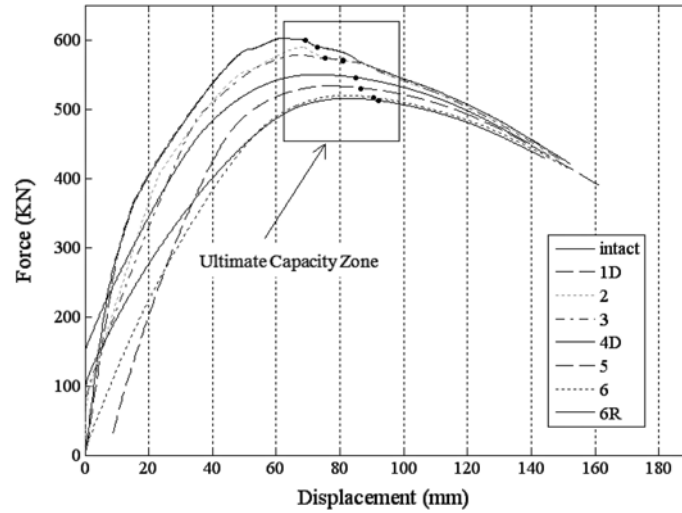


Fig. 8 Pushover curves of the bridge in longitudinal direction following each event

each of the loading events. Pushover analysis did not converge for event 5 in transverse direction and therefore not included in Fig. 7. The selected area in Figs. 7 and 8 pinpoint the zone for which the capacity of the bridge has been reached following individual events, and therefore, the ultimate loads fall inside these zones. The ultimate loads are designated within the zone in Figs. 7 and 8. Capacity loss was defined as the difference between the ultimate capacity following each event and the ultimate capacity of the intact structure. Correlation of the ultimate loading capacity losses against maximum displacements of the deck during each loading event provide further insight into the physical state of the bridge following the progressively increasing seismic loads. This is demonstrated in Figs. 9 and 10 for the longitudinal and transverse directions, respectively. Fig. 9 corresponds to the collective response of the three bents of the bridge. Since the transverse response of the three bents yielded different displacements, the response of bent 2 was selected to represent the transverse behavior of the bridge (Fig. 10). The displacements in the longitudinal direction are resisted by the abutments and despite the effect of the plastic hinging the damages are more pronounced in the lateral direction by way of larger

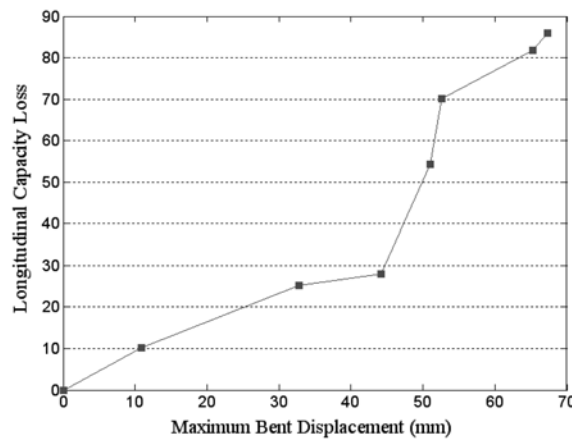


Fig. 9 Loss of capacity in the longitudinal direction

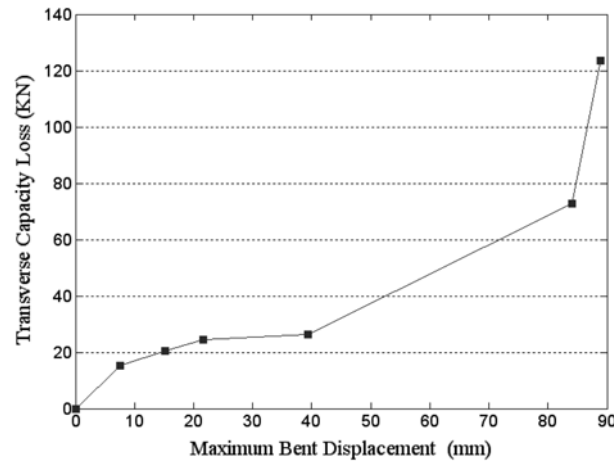


Fig. 10 Loss of capacity in the transverse direction

capacity losses. Instability and collapse in this case occurs in the lateral direction as shown by the sharp increase in the capacity loss for the last events. The measure of damage correlates well with the recorded displacements.

## 6. Conclusions

Scope of the investigation in this study included the application and evaluation of nonlinear finite element analysis in structural health monitoring for post seismic evaluation of a typical highway bridge. The experimental portion of the research involved shake table tests of a four span bridge using the recorded ground motions of the 1994 Northridge earthquake. The objective was to establish a simplified damage assessment technique correlating the residual capacity of the bridge after a seismic event to maximum displacement recorded during the event. The bridge was subjected to progressively increasing amplitudes of the ground motions in order to investigate the efficiency of the method. The nonlinear finite element simulation predicted the bridge bents displacements commensurate with the experimentally measured displacements. A post-event nonlinear static-pushover approach was applied to compute the ultimate capacity of the bridge following an earthquake. The capacity loss in each direction can be introduced as a global structural measure of damage in that direction. This measure of damage was correlated to the maximum displacement recorded during a seismic event.

## Acknowledgements

This project was made possible by a grant from the National Science Foundation, grant number CMS-0523333. The financial support of the Photonics Technology Access Program (PTAP) for the design and acquisition of the special prototype fiber optic sensor interrogation unit is greatly appreciated. The shake table experiments were conducted at the University of Nevada, Reno (UNR) as part of the NSF-NEES project. The cooperation of UNR researchers and staff with this work is greatly acknowledged.

## References

- Ansari, F. (2007), "Practical implementation of optical fiber sensors in civil structural health monitoring", *J. Intel. Mat. Syst. Str.*, **18**(8), 879-889.
- Ansari, F. (2005), *Sensing Issues in Civil Structural Health Monitoring*, Springer Publishing Co., The Netherlands.
- Applied Technology Council (ATC) (2006), *Next-Generation Performance Based Seismic Design Guidelines, Program Plan for New and Existing Buildings*, FEMA-445.
- Applied Technology Council (ATC) (2005), *Improvement of Inelastic Analysis Procedures*, FEMA-440.
- ATC/MCEER (2001), *Recommended LFRD guidelines for the seismic design of highway bridges (2002) Part 1: specifications*, MCEER-02-SP01, MCEER/ATC joint venture, NCHRP 12-49 Project Team.
- Bazant, Z.P. (2005), *Scaling of Structural Strength*, 336 pages, Elsevier.
- Buckle, I.G. (1994), *The Northridge California Earthquake of January 17, 1994: Performance of Highway Bridges*, NCEER-94-0008, National Centre for Earthquake Engineering Research, Buffalo, NY.
- Chaboche, J. (1988), "Continuum damage mechanics. I - General concepts. II - Damage growth, crack initiation, and crack growth", *J. Appl. Mech.-T.*, ASME, **55**, 59-724.
- Davis, P.J. and Rabinowitz, P. (1984), *Methods of Numerical Integration*, 2nd ed., Academic Press, New York.
- Karsan, I.D. and Jirsa, J.O. (1969), "Behavior of concrete under compressive loadings", *J. Struct. Div. ASCE*, **95**(12), 2543-2563.
- Krätzig, W.B. and Petrynab, Y.S. (2005), "Structural damage and life-time estimates by nonlinear FE simulation", *Eng. Struct.*, **27**, 1726-1740.
- Luco, N., Bazzurro, P. and Cornell, C.A. (2004), "Dynamic versus static computation of the residual capacity of a mainshock-damaged building to withstand an aftershock", *Proc. of 13th WCEE*, Paper 2405, Vancouver, B.C., Canada, August 1-6.
- Mander, J., Priestley, N. and Park, R. (1988), "Theoretical stress-strain model for confined concrete", *J. Struct. Eng. ASCE*, **114**(8), 1804-1849.
- Mazzoni, S., McKenna, F. and Fenves, G.L. (2005), *OpenSees Command Language Manual*, Berkeley, CA.
- McKenna, F. and Fenves, G.L. (2000), "An object-oriented software design for parallel structural analysis", *Proc. of the SEI/ASCE Structures Congress*, Philadelphia, PA.
- Nelson, R.B., Saiidi, M.S. and Zadeh, S. (2007), "Experimental evaluation of performance of conventional bridge systems", Report No. CCEER-07-04, Center for Civil Engineering Earthquake Research, University of Nevada, Reno, NV.
- Newmark, N.M. (1959), "A method of computation for structural dynamics", *J. Eng. Mech. Div. ASCE*, **85**, 67-94.
- Wehbe, N. and Saiidi, M. (2003), "User's Manual for RCMC v. 2.0, A Computer Program for Moment-Curvature Analysis of Confined and Unconfined Reinforced Concrete Sections", Report No. CCEER 03-2, Civil Engineering Department, University of Nevada, Reno, NV.
- Zadeh, M.S. and Saiidi, M.S. (2007), "Pre-test analytical studies of NEESR-SG 4-Span bridge model using openses", Report No. CCEER-07-3, Center for Civil Engineering Earthquake Research, University of Nevada, Reno, NV.